ISSN 1070-3284, Russian Journal of Coordination Chemistry, 2017, Vol. 43, No. 6, pp. 373–379. © Pleiades Publishing, Ltd., 2017.
Original Russian Text © N.V. Somov, F.F. Chausov, R.M. Zakirova, V.G. Petrov, M.A. Shumilova, V.A. Aleksandrov, 2017, published in Koordinatsionnaya Khimiya, 2017, Vol. 43, No. 6, pp. 369–375.

Synthesis and Structure of Bis-Hexaaquasodium Bis-Nitrilotris(methylenephosphonato)decaaqua-monohydrohexasodiumlanthanate Trihydrate $[Na(H_2O)_6]_2[LaNa_6H(H_2O)_{10}\{N(CH_2PO_3)_3\}_2] \cdot 3H_2O$

N. V. Somov[a], *, F. F. Chausov[b, c, d], R. M. Zakirova[b], V. G. Petrov[d], M. A. Shumilova[d], and V. A. Aleksandrov[d]

[a]*Lobachevsky National Research University, Nizhny Novgorod, 603950 Russia*
[b]*Udmurt State University, Izhevsk, 426034 Russia*
[c]*Physical-Technical Institute, Ural Branch, Russian Academy of Sciences, Izhevsk, 426000 Russia*
[d]*Institute of Mechanics, Ural Branch, Russian Academy of Sciences, Izhevsk, 426067 Russia*
**e-mail: somov@phys.unn.ru*

Received September 27, 2016

Abstract—A complex salt of nitrilotris(methylenephosphonic acid) with sodium and lanthanum was prepared, isolated, and studied. The salt $[Na(H_2O)_6]_2[LaNa_6H(H_2O)_{10}\{N(CH_2PO_3)_3\}_2] \cdot 3H_2O$ crystallizes in space group $P2_1/c$, $Z = 2$, $a = 11.86630(10)$, $b = 10.55060(10)$, $c = 19.99270(10)$ Å, $\beta = 94.6760°$. The La coordination polyhedron is a virtually regular rhombohedron. The Na atom is coordinated at the vertices of a distorted octahedron. Both ligand molecules chelate the La atom; each PO_3 group forms a La–O–P–O–Na bridge; the ligand denticity is 7.

Keywords: lanthanum, sodium, nitrilotris(methylenephosphonic acid), lanthanum coordination chemistry, clathrochelate, cage complex

DOI: 10.1134/S1070328417060082

INTRODUCTION

Lanthanum with the ground state configuration [Xe]6s25d1 occupies a unique place among transition metals. Being the first in the third d-element row, it simultaneously adjoins the first row of f-elements; the transition energy from the ground state to the excited state [Xe] $6s^24f^1$ is moderate, namely, 15197 cm^{-1} [1]. Therefore, the coordination chemistry of lanthanum is of obvious interest.

The La coordination numbers in complexes most often range from 8 to 10; much more rarely, they are 3–8 or 11 [2, 3]. The coordination polyhedra (CP) of La are usually highly distorted up to full asymmetry [2–4]. Indeed, in mixed-ligand complexes with 1,1,1,5,5,5-hexafluoropentane-2,4-dithionate anion (Hfacac) and 2,2'-bipyridine (2,2-Bipy) [5] and with Hfacac and 4-(2-tetrathiafulvalenyl-ethenyl)pyridine [6], the La atoms have C.N. of 10 (the CP is an asymmetric ten-vertex polyhedron). In the polymeric complex with glycine (Gly), $[La(Gly)_3(H_2O)_4]_n(ClO_4)_{3n}$ [7], the La atom is also ten-coordinate by the oxygen atoms of the Gly molecule and water and forms an asymmetric CP. The replacement of the perchlorate anions by chlorides decreases the $C.N._{La}$ in $[La(Gly)_3(H_2O)_2]_nCl_{3n} \cdot nH_2O$ to nine; the CP is also asymmetric [8]. A higher CP symmetry is inherent in La complexes with inorganic ligands. In the $Na_2(NH_4)_7[La(W_5O_{18})_2] \cdot 16H_2O$ complex, the La atom is coordinated by eight oxygen atoms of the polyoxotungstate anions at the vertices of a regular tetragonal antiprism (Thomson cube) [9]. The symmetry of the CP is determined in this case by the ligand stereochemistry.

The considerable HOMO–LUMO gap for La complexes (e.g., 2.778 eV for $[Ln(C_3H_5)Cp(OCH_3)]$, where Cp is cyclopentadienyl [10]) is responsible for the La tendency to form coordination bonds with the hardest ligands [11, 12]. This is manifested, in particular, in the considerable difference between the La–O and La–N bond lengths in the presence of N- and O-donor centers in the ligand molecule [13]. For example, in the above-mentioned Hfacac and 2,2-Bipy complex [5], the La–O distances are 2.524(3)–2.557(2) and the La–N distances are 2.771(3)–2.773(3) Å. In many cases, N-donor centers of the ligands are not incorporated in the La coordination sphere. In the La complex with Hfacac and 4-(2-tetrathiafulvalenyl-ethenyl)pyridine [6], the La–N distances reach 4.409(8) Å, while in the polymer complexes with Gly [7, 8], the La–N distances are even longer. It is pertinent to continue the studies of the competition between the N- and O-donor centers in the La coordination.

Aminopolyphosphonic acids are a vivid example of ligands that have both N- and O-donor centers and are capable of a variety of binding motifs. For example, nitrilotris(methylenephosphonic acid) $N(CH_2PO_3)_3H_6$ (NTP) finds a wide use in steel corrosion inhibitors [14, 15] and bactericidal agents [16]. Nevertheless, the structure and properties of La complexes with NTP have not been adequately studied. The reaction of aqueous solutions of $La(NO_3)_3 \cdot 6H_2O$ and NTP gave the $LaH_3NTP \cdot nH_2O$ complex at pH 0.2 [17] and $La_2HNTP \cdot NO_3 \cdot nH_2O$ at pH 7.5 [18]; the structures of the products were not studied. The $LaH_3NTP \cdot 5H_2O$ complex was isolated and investigated by physicochemical methods [19]. According to powder X-ray diffraction, this complex is crystalline, but the crystal structure remains unknown. The nitrogen atom of the NTP molecule in this complex is protonated, as shown by IR spectroscopy. According to thermogravimetric analysis, the N–C–P bonds are broken above 400°C.

This communication describes the synthesis and structure of the sodium salt of the NTP complex with lanthanum.

EXPERIMENTAL

Synthesis of bis-hexaaquasodium bis-[nitrilotris(methylenephosphonato)decaaquamonohydro-hexasodiumlanthanate] trihydrate $[Na(H_2O)_6]_2$-$[LaNa_6H(H_2O)_{10}\{N(CH_2PO_3)_3\}_2] \cdot 3H_2O$ (I). Lanthanum hydroxide freshly precipitated by excess NaOH from a solution of analytical grade $La(NO_3)_3 \cdot 6H_2O$ (4.33 g, 0.01 mol) and washed with water to a neutral medium was quantitatively transferred into an aqueous solution containing twice- recrystallized NTP (6.00 g, 0.02 mol) and reagent grade NaOH (3.20 g, 0.08 mol). The reaction mixture was stirred until a homogeneous transparent solution formed (pH 8.8) and filtered. Slow evaporation of the solvent gave crystals of **I** as transparent colorless monoclinic prisms. The crystals thus obtained were washed with water with addition of 45% ethanol.

X-ray diffraction. The primary fragment of the structure of **I** was determined by the direct method, the positions of atoms were derived from electron density maps. The non-hydrogen atom parameters were refined in the anisotropic approximation by the least-squares method on $|F|^2$. The hydrogen atom positions were refined in the isotropic approximation. Some hydrogen atom parameters were fixed during the refinement. One proton, which belonged to the $[LaNa_6H(H_2O)_{10}\{N(CH_2PO_3)_3\}_2]^{2-}$ ion according to X-ray diffraction data, could not be located. The crystallographic parameters and X-ray experiment and structure refinement details for **I** are summarized in Table 1.

The X-ray diffraction data for **I** are deposited with the Cambridge Crystallographic Data Centre (CCDC no. 1493172; http://www.fiz-karlsruhe.de/request_or_deposited_data.html).

Thermogravimetric analysis of **I** was carried out on a Shimadzu DTG-60H automatic derivatograph in the 30–500°C temperature range at a heating rate of 3 K/min (argon).

Powder X-ray diffraction study of the thermal decomposition products of **I** was carried out on a DRON-6 two-circle diffractometer (CoK_α radiation, $\lambda = 1.79$ Å) in the 2θ range of 6°–100°.

The IR spectra of **I** and the products formed upon its thermal decomposition were measured for KBr pellets (test compound, 1 mg; KBr, 250 mg) on a FSM-1201 FT IR spectrometer in the 450–5000 cm^{-1} range.

The Raman spectrum of the single crystal of **I** was recorded on a Centaur U-HR microscope/microspectrometer in the 473–573 nm range with laser excitation at 473 nm.

RESULTS AND DISCUSSION

Figure 1 shows the structure of the La complex ion in compound **I**. The interatomic distances and bond angles are summarized in Table 2. It can be seen in Fig. 1a that the La atom (at the inversion center) is coordinated by two NTP molecules. All phosphonate groups in the NTP molecules are fully deprotonated $\left(-PO_3^{2-}\right)$, as indicated by similar distances (aver. P–O, 1.5236(74) Å) for all oxygen atoms (protonation of the O atom would increase the P–O distance by ~0.06 Å [25–28]). As can be seen in Fig. 1b, two trigonal pseudosymmetric NTP molecules occur in the staggered conformation relative to each other, i.e. one of the two ligand molecules is rotated by 60° relative to the other molecule around the axis passing through nitrogen atoms. In each PO_3 group, one O atom (P–O, 1.5330(14)–1.5350(13) Å) is coordinated to La and the Na atoms, the second O atom (P–O, 1.5162(14)–1.5224(14) Å) is coordinated to only Na, and the third one (P–O, 1.5158(14)–1.5184(14) Å) is not involved in the metal coordination and is only hydrogen-bonded to solvation water molecules. The nitrogen atom is deprotonated; the LaNC bond angles (aver. 108.83(18)°) are almost equal to the ideal tetrahedral angle, which is indicative of nitrogen quaternization and participation in the coordination to La. Lanthanum coordination to two NTP molecules results in closure of six five-membered La–N–C–P–O rings sharing La–N bonds and six eight-membered La–O–P–C–N–C–P–O rings. The La–N–

Table 1. Crystallographic parameters and X-ray experiment and structure refinement details for **I**

Parameter	Value
Molecular formula	$C_6H_{63}N_2O_{43}P_6Na_8La$
M	1360.23
System; space group; Z	Monoclinic; $P2_1/c$; 2
a, Å	11.86630(10)
b, Å	10.55060(10)
c, Å	19.99270(10)
β, deg	94.6760(10)
V, Å^3	2494.69(3)
ρ(calcd.), g/cm^3	1.811
Radiation; λ, Å	MoK_α; 0.71073
μ, mm^{-1}	1.229
T, K	293(2)
Sample size, mm	0.16 × 0.115 × 0.099
Diffractometer	Xcalibur, Sapphire III, Gemini S
Scan mode	ω
Absorption corrections, T_{min}/T_{max}	Analytical [20], 0.803/0.851
$\theta_{min}/\theta_{max}$, deg	3.384/30.506
Limits of h, k, l	$-16 \le h \le 16, -15 \le k \le 14, -28 \le l \le 28$
Number of reflections measured//	47395
independent (N_1) (R_{int})	7593 (0.0277)
Number of reflections with $I > 2\sigma(I)$ (N_2)	7095
Refinement method	Full-matrix least-squares on F^2
Number of parameters /restraints	438/46
S	1.092
R_1/wR_1 for N_1	0.0288/0.071
R_1/wR_1 for N_2	0.0261/0.0696
$\Delta\rho_{min}/\Delta\rho_{max}$, e/Å^3	−0.557/0.967
Programs	CrysAlisPro [21], SHELX-2014 [22], WinGX [23], VESTA 3.0 [24]

C–P–O rings have an envelope conformation: the P–O–La–N torsion angles are 4.86(3)°–8.30(3)°, the C atom is "broken out" of the ring plane.

The La atom is coordinated at the vertices of a nearly regular rhombohedron with an edge of 2.999(77) Å. The six rhombohedron vertices closest to the center are occupied by O atoms, while the two remote vertices located on the three-fold inversion axis of the rhombohedron are occupied by N atoms. The CP of La can also be represented as a cube elongated along the body diagonal with two vertices located on this diagonal being occupied by nitrogen atoms. This highly symmetric CP is unusual for La; to our knowledge, no data on La complexes with a regular rhombohedral coordination have been reported.

The average La–O distance (2.457(8) Å) is consistent with the sum of the La and O covalent radii (1.80 and 0.63 Å) [29]. However, according to [30], the covalent radii of La and O are 2.07(8) and 0.66(2) Å, respectively, which does not agree with the crystal chemical data for **I**. The summation of La^{3+} (C.N. 8) and O^{2-} (C.N. 3) ionic radii (according to [31], 1.16 and 1.36 Å, respectively) also gives an overestimated La–O distance. The La–N distance (2.9752(15) Å) is markedly greater than the sum of La and N radii taken from any of the three sources [29–31], where the nitrogen covalent radius is 0.71 and ionic radius is 1.46 Å. The difference between the La–N and La–O distances is, on average, 0.518(8) Å.

The crystal packing of complex **I** is shown in Fig. 2. The outer coordination sphere of **I** is composed of eight sodium ions located in pairs symmetrically with respect to the inversion center. Each Na$^+$ ion is coordinated by six oxygen atoms. Six Na$^+$ ions in the

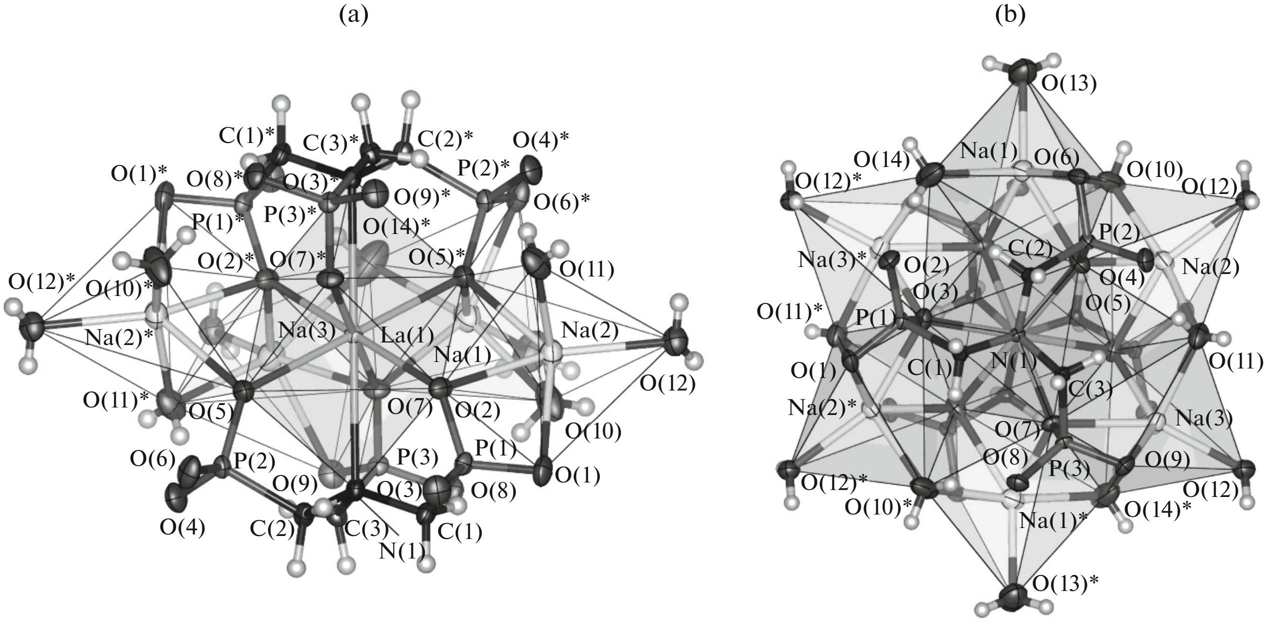

Fig. 1. Structure of the $[LaNa_6H(H_2O)_{10}\{N(CH_2PO_3)_3\}_2]^{2-}$ complex ion (symmetry codes: $-x, -y, -z$): (a) projection onto the (101) plane; (b) projection onto the $(30\bar{2})$ plane.

Na(1), Na(2), and Na(3) sites linked to the PO_3 oxygen atoms and to ten water molecules of crystallization close a corrugated ring surrounding the inner coordination sphere of the complex. The steric strain in the oxygen environment of these Na^+ ions resulting from this configuration induces a strong distortion of the octahedral geometry of the oxygen environment. The crystal packing of complex **I** is formed by ribbons of $[LaNa_6H(H_2O)_{10}\{N(CH_2PO_3)_3\}_2]^{2-}$ complex ions linked by bridging O(12) water molecules. These ribbons lie in the $(30\bar{2})$ plane and are stretched along the *y* axis. Two Na^+ ions are located above and below the plane of these ribbons in the Na(4) sites, which are symmetrical relative to the screw axis running along each ribbon. These Na^+ ions are surrounded by water molecules of crystallization located at the vertices of a slightly distorted octahedron and are hydrogen-bonded to the ligand phosphonate groups. This packing has a lot of voids, which accounts for the relatively low density of the crystal of **I** (1.811 g/cm^3). The crystal packing voids accommodate three solvation water molecules hydrogen-bonded to the NTP phosphonate groups. The positions of these water molecules are disordered and are characterized by fractional occupancies: O(21*A*)—0.440(2), O(21*B*)—0.365(2), O(21C)—0.195(2), and O(22)—1/2.

The molecular vibrational spectra of **I** are shown in Fig. 3. The bands in the 170–350 cm^{-1} range correspond to the mutual vibrations of the crystal subunits (complex ions). The broad asymmetric band at 404 cm^{-1} and a group of bands at 493, 571, and 635 cm^{-1} are due to the δ(OPO) modes for the bonds with different metal atoms. The high symmetry of the $[LaNa_6H(H_2O)_{10}\{N(CH_2PO_3)_3\}_2]^{2-}$ ion is manifested as alternative selection of these vibration modes. The group of bands at 760, 790, 857, and 912 cm^{-1}, which are present in both Raman and IR spectra, refer to the N–C–P bonds. The ν(P–O) mode is responsible for the bands at 970, 990, and 1002 cm^{-1} and for the broad bands with intricate structure at 1063, 1104, and 1124 cm^{-1}, which obey the alternative selection rules. The localized P–O π-bond accounts for the 1255 cm^{-1} band, which is strong in the Raman spectrum and weak in the IR spectrum; this is consistent with the centrally symmetrical position of the P(1)–O(3), P(2)–O(4), and P(3)–O(8) bonds. The other bands in the spectrum are as follows (cm^{-1}): 1435 δ(CH_2), 1500–1600 δ(H_2O), 2730, 2840, 2880, 2978 ν(CH_2), 3376, 3448, 3521, and 3569 ν(H_2O).

The thermal decomposition of **I** occurs in several stages (Fig. 4). In the 30–175°C range, water molecules are eliminated; compound **I** is dehydrated in several stages owing to its complicated structure. The broad asymmetric endotherm and weight loss peak in the 30–90°C range correspond to the elimination of 17 H_2O molecules. Apparently, these molecules include the solvation water molecules from the O(21*A*)–O(21*C*) and O(22) sites and the water molecules from the O(13) and O(15)–O(20) sites coordinated to only one Na^+ ion. In the 90–130°C range, six more water molecules are eliminated; these are molecules that occupy the bridging positions between two

Table 2. Interatomic distances (d) and bond angles (ω) in structure **I**

Bond	d, Å	Bond	d, Å	Bond	d, Å
La(1)–N(1)	2.9752(15)	C(1)–P(1)	1.8184(18)	P(2)–O(4)	1.5158(14)
La(1)–O(2)	2.4649(13)	C(2)–P(2)	1.8157(18)	P(2)–O(5)	1.5330(14)
La(1)–O(5)	2.4621(13)	C(3)–P(3)	1.8175(18)	P(2)–O(6)	1.5224(14)
La(1)–O(7)	2.4462(12)	P(1)–O(1)	1.5162(14)	P(3)–O(7)	1.5350(13)
N(1)–C(1)	1.474(2)	P(1)–O(2)	1.5334(13)	P(3)–O(8)	1.5184(14)
N(1)–C(2)	1.485(2)	P(1)–O(3)	1.5179(14)	P(3)–O(9)	1.5207(14)
N(1)–C(3)	1.479(2)				

Bond	d, Å	Bond	d, Å
Na(1)–O	2.374(3)–2.6280(18)	Na(3)–O	2.3795(17)–2.697(3)
Na(2)–O	2.3844(19)–2.570(2)	Na(4)–O	2.369(3)–2.547(3)

Angle	ω, deg	Angle	ω, deg	Angle	ω, deg
N(1)La(1)O(2)	64.22(6)	O(1)P(1)C(1)	106.06(12)	O(1)P(1)O(2)	111.08(13)
N(1)La(1)O(5)	64.00(6)	O(2)P(1)C(1)	104.18(12)	O(1)P(1)O(3)	113.28(13)
N(1)La(1)O(7)	64.69(6)	O(3)P(1)C(1)	110.19(13)	O(2)P(1)O(3)	111.52(13)
N(1)La(1)O(2)*	115.78(6)	O(4)P(2)C(2)	109.40(13)	O(4)P(2)O(5)	112.22(13)
N(1)La(1)O(5)*	116.00(6)	O(5)P(2)C(2)	104.59(12)	O(4)P(2)O(6)	112.85(13)
N(1)La(1)O(7)*	115.31(6)	O(6)P(2)C(2)	106.69(12)	O(5)P(2)O(6)	110.59(13)
O(2)La(1)O(5)	103.20(7)	O(7)P(3)C(3)	104.80(12)	O(7)P(3)O(8)	111.52(13)
O(2)La(1)O(7)	103.24(7)	O(8)P(3)C(3)	110.02(13)	O(7)P(3)O(9)	110.70(13)
O(5)La(1)O(7)	101.31(7)	O(9)P(3)C(3)	106.13(12)	O(8)P(3)O(9)	113.19(13)

Angle	ω, deg	Angle	ω, deg
ONa(1)O	130.51(10)–164.77(12) 57.48(7)–122.07(11)	ONa(3)O	132.78(9)–160.31(10) 59.57(8)–122.70(10)
ONa(2)O	132.85(9)–159.14(11) 59.74(8)–126.37(10)	ONa(4)O	168.26(12)–176.42(12) 80.25(11)–100.69(10)

* Symmetry codes: $-x$, $-y$, $-z$.

Na^+ ions. The complete dehydration of **I** (elimination of the last two water molecules) takes place at 140–175°C. During the dehydration, the crystal structure of the sample is completely destroyed; therefore, we were unable to determine the structure of the dehydration product. In the 175–345°C range, the gradual loss of the sample weight corresponds to elimination of $1/2H_2O$, while at 345–400°C, the weight loss corresponds to elimination of one more H_2O molecule, apparently, as a result of condensation of proximate phosphonic groups as shown below

$$2R{-}P(O)(OH)_2 \\ \rightarrow R{-}P(O)(OH){-}O{-}P(O)(OH){-}R + H_2O.$$

The sharp change in the course of the thermal curve in this region is attributable to a change in the sample heat capacity. In the 400–480°C range, the weight loss of the sample corresponds to the elimination of two N atoms and two methylene groups accompanied by intensive heat evolution. This is consistent with the previously noted [19] destruction of the N–C–P skeleton above 400°C. The IR spectrum of the thermal decomposition products of **I** (Fig. 3, *3*) shows the characteristic lines of lanthanum orthophosphate $LaPO_4$ [32, 33] (cm^{-1}: 557, 574, 618 δ(O–P–O), 992, 1055 ν(PO_3)); lanthanum monohydrodiphosphate $LaHP_2O_7$ [34] (cm^{-1}: 753, 950 ν(P–O–P)), lanthanum trimetaphosphate

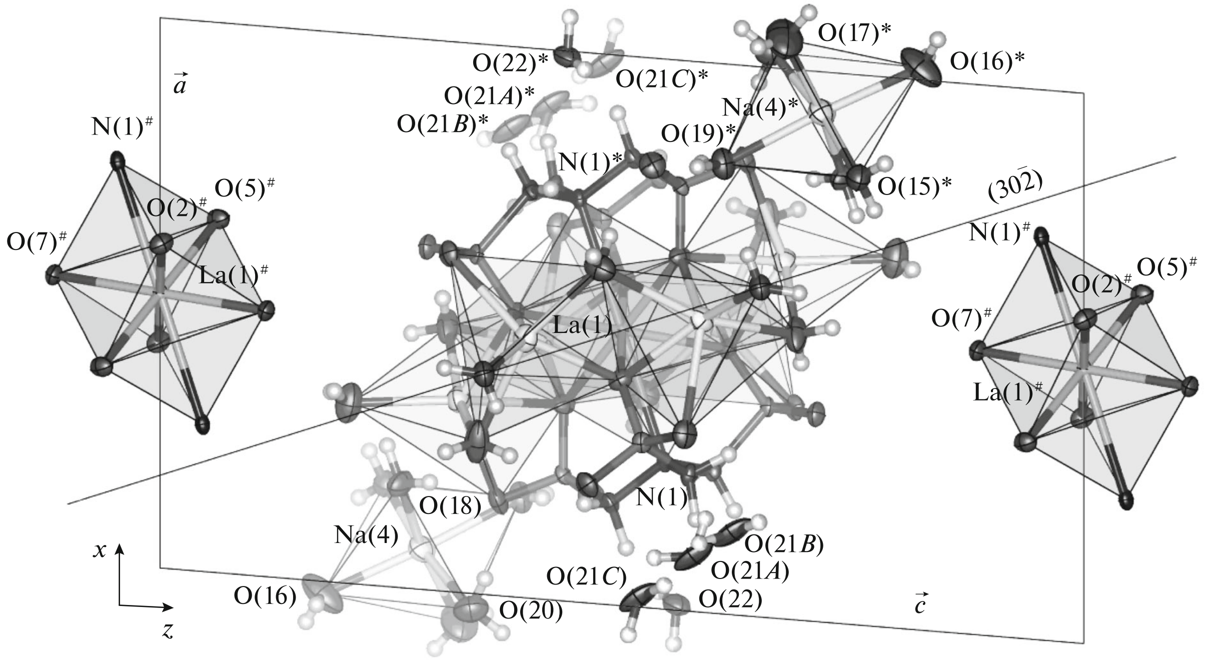

Fig. 2. Crystal packing of **I** (projection onto the (010) plane; symmetry codes: * $-x$, $-y$, $-z$; # $-x$, $y + 1/2$, $-z + 1/2$). The $(30\bar{2})$ plane and the cross-section of the ribbon composed of $[LaNa_6H(H_2O)_{10}\{N(CH_2PO_3)_3\}_2]^{2-}$ ions and located in this plane are shown. The coordination environment of La in the symmetry-equivalent positions La(1)# is partly omitted for the sake of simplicity.

$La(PO_3)_3$ [35, 36] (cm^{-1}: 732, 917 ν(P–O–P), 1120 ν(PO_3)), and sodium metaphosphate $NaPO_3$ [37, 38] (cm^{-1}: 485, 523 δ(O–P–O), 1006 ν(PO_3), 1315 ν(P=O)). Powder X-ray diffraction analysis of the

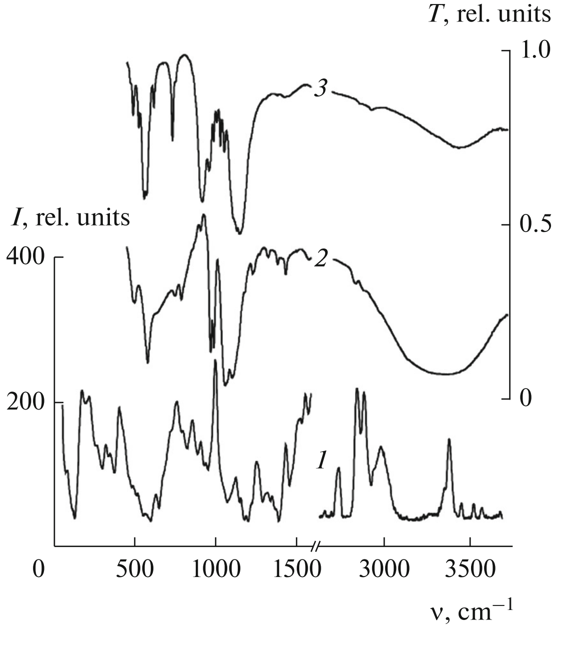

Fig. 3. (*1*) Raman spectrum of the single crystal of **I**; (*2*) IR spectrum of **I** and (*3*) IR spectra of the thermal decomposition of **I** in argon.

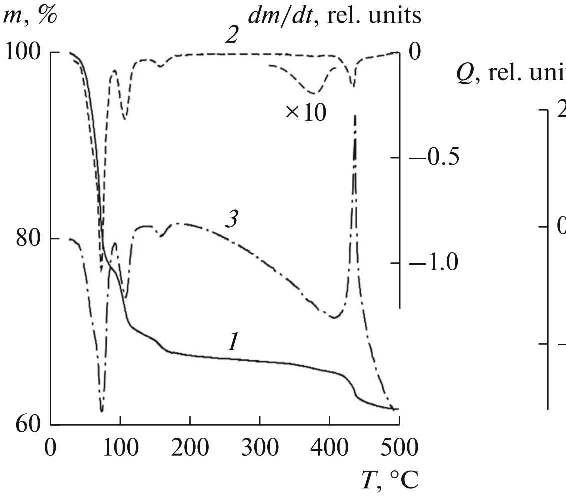

Fig. 4. Thermogravimetric curves of **I** in argon: (*1*) sample weight *m*, (*2*) derivative *dm*/*dt*, and (*3*) heat *Q* vs. temperature *T*.

products of thermal decomposition of **I** attests that $LaPO_4$ occurs as monazite (space group $P2_1/n$) [39].

ACKNOWLEDGMENTS

This work was carried out in terms of the government order no. 2014/134 for work in the field of scientific research within the basic part of the order (project code 2312).

REFERENCES

1. Safronova, M.S., Safronova, U.I., and Clark, C.W., *Phys. Rev. A*, 2015, vol. 91, p. 022504.
2. *Comprehensive Coordination Chemistry*, Wilkinson, G., Gillard, R.D., McCleverty, J.A., Eds., Oxford: Pergamon, 1987, vol. 3.
3. *Comprehensive Coordination Chemistry II*, Mc. Cleverty, J.A., and Meyer, T.J., Eds., Elsevier, 2003, vol. 3.
4. *Rare Earth Coordination Chemistry. Fundamentals and Applications*, Chunhui, H., Ed., New York: Wiley, 2010.
5. Van Staveren, D.R., Van Albada, G.A., Haasnoot, J.G., et al., *Inorg. Chim. Acta*, 2001, vol. 315, no. 2, p. 163.
6. Pointillart, F., Maury, O., Le Gal, Y., et al., *Inorg. Chem.*, 2009, vol. 48, no. 15, p. 7421.
7. Ma, A., Li, L., Lin, Y., and Xi, S., *J. Coord. Chem.*, 1994, vol. 33, no. 1, p. 59.
8. Gao, S.-L., Li, Y.-Z., Ren, F., et al., *Acta Crystallogr., Sect. E: Struct. Rep. Online*, 2002, vol. 58, no. 5 p. m234.
9. Paz, F.A.A., Balula, M.S.S., and Cavaleiro, A.M.V., *Acta Crystallogr., Sect. E: Struct. Rep. Online*, 2005, vol. 61, p. i28.
10. Schinzel, S., Bindl, M., Visseaux, M., and Chermette, H., *J. Phys. Chem. A*, 2006, vol. 110, p. 11324.
11. Pearson, R.G., *J. Chem. Educ.*, 1999, vol. 76, no. 2, p. 267.
12. Geerlings, P., De Proft, F., and Langenaeker, W., *Chem. Rev.*, 2003, vol. 103, no. 5, p. 1793.
13. Porai-Koshits, M.A., Polynova, T.N., and Shkol'nikova, L.M., *Ross. Khim. Zh.*, 1984, vol. 29, no. 3, p. 43.
14. Kuznetsov, Yu.I., *Usp. Khim.*, 2004, vol. 73, no. 1, p. 79.
15. Chausov, F.F., Shabanova, I.N., Kazantseva, I.S., Naimushina, E.A., *Izv. Ross. Akad. Nauk., Ser. Fiz.*, 2014, vol. 78, no. 4, p. 436.
16. Somov, N.V. and Chausov, F.F., *Crystallogr. Rep.*, 2016, vol. 61, no. 1, p. 39.
17. Khramov, V.P. and Kol'tsov, A.A. *Izv. Vyssh. Ucheb. Zaved., Ser. Khim. Khim. Tekhnol.*, 1974, vol. 17, p. 1295.
18. Khramov V.P. and Kol'tsov A.A., *Izv. Vyssh. Ucheb. Zaved., Ser. Khim. Khim. Tekhnol.,* 1975, vol. 18, p. 710.
19. Tananaev, I.V., Tereshin, G.S., Kuznetsova, O.B., et al., *Zh. Neorg. Khim.*, 1981, vol. 26, no. 1, p. 276.
20. Clark, R.C. and Reid, J.S., *Acta Crystallogr., Sect. A: Found. Crystallogr.*, 1995, vol. 51, p. 887.
21. *CrysAlisPro 1.171.38.41*, Rigaku Oxford Diffraction, Oxford, 2015.
22. Sheldrick, G.M., *Acta Crystallogr., Sect. A: Found. Crystallogr.*, 2008, vol. 64, p. 112.
23. Farrugia, L.J., *J. Appl. Crystallogr.*, 1999, vol. 32, p. 837.
24. Momma, K. and Izumi, F., *J. Appl. Crystallogr.*, 2011, vol. 44, p. 1272.
25. Somov, N.V., Chausov, F.F., Zakirova, R.M., et al., *Russ. J. Coord. Chem.*, 2015, vol. 41, no. 10, p. 688.
26. Somov, N.V., Chausov, F.F., Zakirova, R.M., and Fedotova, I.V., *Russ. J. Coord. Chem.*, 2015, vol. 41, no. 12, p. 798.
27. Somov, N.V., Chausov, F.F., Zakirova, R.M., et al., *Crystallogr. Rep.*, 2015, vol. 60, no. 6, p. 853.
28. Somov, N.V., Chausov, F.F., Zakirova, R.M., and Fedotova, I.V., *Crystallogr. Rep.*, 2016, vol. 61, no. 2, p. 216.
29. Pyykkö, P. and Atsumi, M., *Chem.-Eur. J.*, 2009, vol. 15, p. 186.
30. Cordero, B., Gómez, V., Platero-Prats, A.E., et al., *Dalton Trans.*, 2008, no. 21, p. 2832.
31. Shannon, R.D., *Acta Crystallogr., Sect. A: Cryst. Phys., Diffr., Theor. Gen. Crystallogr.*, 1976, vol. 32, p. 751.
32. Savchyn, P., Karbovnyk, I., Vistovskyy, V., Voloshinovskii, A., Pankratov, V., et al., *J. Appl. Phys.*, 2012, vol. 112, p. 124309.
33. Patil, Y.S., Chaudhari, K.G., Murthy, K.V.R., and Poornachandra Rao, N.V., *Arch. Appl. Sci. Res.*, 2012, vol. 4, no. 2, p. 757.
34. Ben Moussa, S., Ventemillas, S., Cabeza, A., et al., *J. Solid State Chem.*, 2004, vol. 177, p. 2129.
35. Guojing, Z., Rong, Y., Shashi, V., et al., *Solid State Ionics*, 2008, vol. 178, p. 1811.
36. Matuszewski, J., Kropiwmicka, J., and Znamieroska, T., *J. Solid State Chem.*, 1988, vol. 75, p. 285.
37. Ogden, J.S. and Williams, S.J., *J. Chem. Phys.*, 1980, vol. 73, no. 4, p. 2007.
38. Bencivenni, L. and Gingerich, K.A., *J. Mol. Struct.*, 1983, vol. 98, p. 195.
39. Ni, Y., Hughes, J.M., and Mariano, A.N., *Am. Mineral.*, 1995, vol. 80, p. 21.

Translated by Z. Svitanko